Spectro-angular light scattering measurements of individual microscopic objects

JaeHwang Jung and YongKeun Park*

Department of Physics, Korea Advanced Institute of Science and Technology, Daejeon 305-701, South Korea
*yk.park@kaist.ac.kr

Abstract: The spectro-angular light scattering measurements of individual microscopic objects are presented. Using spectroscopic quantitative phase microscopy and Fourier transform light scattering, the 2D angle-resolved light scattering intensity and phase patterns are measured in a spectral range of 450-750 nm and an angular range of –70-70°. The spectro-angular light scattering measurements of individual polystyrene beads are demonstrated with high sensitivity and precision.

OCIS codes: (290.5820) Scattering measurements; (290.5850) Scattering, particles; (180.3170) Interference microscopy.

References and links

1. H. C. d. Hulst, *Light Scattering by Small Particles*, Structure of Matter Series (Wiley, 1957).
2. N. N. Boustany, S. A. Boppart, and V. Backman, "Microscopic imaging and spectroscopy with scattered light," Annu. Rev. Biomed. Eng. **12**(1), 285–314 (2010).
3. A. Wax, M. G. Giacomelli, T. E. Matthews, M. T. Rinehart, F. E. Robles, and Y. Zhu, "Optical spectroscopy of biological cells," Adv. Opt. Photonics **4**(3), 322–378 (2012).
4. H. Ding, Z. Wang, F. Nguyen, S. A. Boppart, and G. Popescu, "Fourier transform light scattering of inhomogeneous and dynamic structures," Phys. Rev. Lett. **101**(23), 238102 (2008).
5. G. Popescu, *Quantitative Phase Imaging of Cells and Tissues* (McGraw-Hill, 2011).
6. K. Lee, K. Kim, J. Jung, J. H. Heo, S. Cho, S. Lee, G. Chang, Y. J. Jo, H. Park, and Y. K. Park, "Quantitative phase imaging techniques for the study of cell pathophysiology: from principles to applications," Sensors **13**(4), 4170–4191 (2013).
7. H. Ding, F. Nguyen, S. A. Boppart, and G. Popescu, "Optical properties of tissues quantified by Fourier-transform light scattering," Opt. Lett. **34**(9), 1372–1374 (2009).
8. H. Ding, E. Berl, Z. Wang, L. J. Millet, M. U. Gillette, J. Liu, M. Boppart, and G. Popescu, "Fourier transform light scattering of biological structure and dynamics," IEEE J. Sel. Top. Quantum Electron. **16**(4), 909–918 (2010).
9. Y. Park, C. A. Best-Popescu, R. R. Dasari, and G. Popescu, "Light scattering of human red blood cells during metabolic remodeling of the membrane," J. Biomed. Opt. **16**(1), 011013 (2011).
10. H. Ding, L. J. Millet, M. U. Gillette, and G. Popescu, "Actin-driven cell dynamics probed by Fourier transform light scattering," Biomed. Opt. Express **1**(1), 260–267 (2010).
11. H. Yu, H. Park, Y. Kim, M. W. Kim, and Y. Park, "Fourier-transform light scattering of individual colloidal clusters," Opt. Lett. **37**(13), 2577–2579 (2012).
12. C. Cho, H. Kim, S. Jeong, S.-W. Baek, J.-W. Seo, D. Han, K. Kim, Y. Park, S. Yoo, and J.-Y. Lee, "Random and V-groove texturing for efficient light trapping in organic photovoltaic cells," Sol. Energy Mater. Sol. Cells **115**, 36–41 (2013).
13. Y. Liu, X. Li, Y. L. Kim, and V. Backman, "Elastic backscattering spectroscopic microscopy," Opt. Lett. **30**(18), 2445–2447 (2005).
14. W. J. Cottrell, J. D. Wilson, and T. H. Foster, "Microscope enabling multimodality imaging, angle-resolved scattering, and scattering spectroscopy," Opt. Lett. **32**(16), 2348–2350 (2007).
15. Z. J. Smith and A. J. Berger, "Validation of an integrated Raman- and angular-scattering microscopy system on heterogeneous bead mixtures and single human immune cells," Appl. Opt. **48**(10), D109–D120 (2009).
16. T. Rothe, M. Schmitz, and A. Kienle, "Angular and spectrally resolved investigation of single particles by darkfield scattering microscopy," J. Biomed. Opt. **17**(11), 117006 (2012).
17. W. Choi, C.-C. Yu, C. Fang-Yen, K. Badizadegan, R. R. Dasari, and M. S. Feld, "Field-based angle-resolved light-scattering study of single live cells," Opt. Lett. **33**(14), 1596–1598 (2008).
18. T. R. Hillman, S. A. Alexandrov, T. Gutzler, and D. D. Sampson, "Microscopic particle discrimination using spatially-resolved Fourier-holographic light scattering angular spectroscopy," Opt. Express **14**(23), 11088–11102 (2006).

#204055 - $15.00 USD Received 2 Jan 2014; revised 8 Feb 2014; accepted 9 Feb 2014; published 13 Feb 2014

19. I. Itzkan, L. Qiu, H. Fang, M. M. Zaman, E. Vitkin, I. C. Ghiran, S. Salahuddin, M. Modell, C. Andersson, L. M. Kimerer, P. B. Cipolloni, K. H. Lim, S. D. Freedman, I. Bigio, B. P. Sachs, E. B. Hanlon, and L. T. Perelman, "Confocal light absorption and scattering spectroscopic microscopy monitors organelles in live cells with no exogenous labels," Proc. Natl. Acad. Sci. U. S. A. **104**(44), 17255–17260 (2007).
20. D. Fu, W. Choi, Y. Sung, S. Oh, Z. Yaqoob, Y. Park, R. R. Dasari, and M. S. Feld, "Ultraviolet refractometry using field-based light scattering spectroscopy," Opt. Express **17**(21), 18878–18886 (2009).
21. J.-H. Jung, J. Jang, and Y. Park, "Spectro-refractometry of individual microscopic objects using swept-source quantitative phase imaging," Anal. Chem. **85**(21), 10519–10525 (2013).
22. Y. Jang, J. Jang, and Y. Park, "Dynamic spectroscopic phase microscopy for quantifying hemoglobin concentration and dynamic membrane fluctuation in red blood cells," Opt. Express **20**(9), 9673–9681 (2012).
23. Y. Park, T. Yamauchi, W. Choi, R. Dasari, and M. S. Feld, "Spectroscopic phase microscopy for quantifying hemoglobin concentrations in intact red blood cells," Opt. Lett. **34**(23), 3668–3670 (2009).
24. H. Pham, B. Bhaduri, H. Ding, and G. Popescu, "Spectroscopic diffraction phase microscopy," Opt. Lett. **37**(16), 3438–3440 (2012).
25. F. E. Robles, C. Wilson, G. Grant, and A. Wax, "Molecular imaging true-colour spectroscopic optical coherence tomography," Nat. Photonics **5**(12), 744–747 (2011).
26. S. K. Debnath and Y. Park, "Real-time quantitative phase imaging with a spatial phase-shifting algorithm," Opt. Lett. **36**(23), 4677–4679 (2011).
27. J.-P. Schäfer, "Implementierung und Anwendung analytischer und numerischer Verfahren zur Lösung der Maxwellgleichungen für die Untersuchung der Lichtausbreitung in biologischem Gewebe," (Ulm, Universität Ulm, Diss., 2011).
28. Y. Park, G. Popescu, K. Badizadegan, R. R. Dasari, and M. S. Feld, "Fresnel particle tracing in three dimensions using diffraction phase microscopy," Opt. Lett. **32**(7), 811–813 (2007).
29. W. W. Tscharnuter, "Mobility measurements by phase analysis," Appl. Opt. **40**(24), 3995–4003 (2001).
30. K. Lee, H.-D. Kim, K. Kim, Y. Kim, T. R. Hillman, B. Min, and Y. Park, "Synthetic Fourier transform light scattering," Opt. Express **21**(19), 22453–22463 (2013).
31. S. Cho, S. Kim, Y. Kim, and Y. Park, "Optical imaging techniques for the study of malaria," Trends Biotechnol. **30**(2), 71–79 (2012).
32. M. Kinnunen, A. Kauppila, A. Karmenyan, and R. Myllylä, "Effect of the size and shape of a red blood cell on elastic light scattering properties at the single-cell level," Biomed. Opt. Express **2**(7), 1803–1814 (2011).
33. H. Byun, T. R. Hillman, J. M. Higgins, M. Diez-Silva, Z. Peng, M. Dao, R. R. Dasari, S. Suresh, and Y. Park, "Optical measurement of biomechanical properties of individual erythrocytes from a sickle cell patient," Acta Biomater. **8**(11), 4130–4138 (2012).
34. S. Lee and W. Lu, "Using elastic light scattering of red blood cells to detect infection of malaria parasite," IEEE Trans. Biomed. Eng. **59**(1), 150–155 (2012).
35. A. Anand, V. Chhaniwal, N. Patel, and B. Javidi, "Automatic identification of malaria-infected RBC with digital holographic microscopy using correlation algorithms," IEEE Photonics J. **4**(5), 1456–1464 (2012).
36. K. Kim and Y. Park, "Fourier transform light scattering angular spectroscopy using digital inline holography," Opt. Lett. **37**(19), 4161–4163 (2012).
37. Y. Kim, J. Jeong, J. Jang, M. W. Kim, and Y. Park, "Polarization holographic microscopy for extracting spatio-temporally resolved Jones matrix," Opt. Express **20**(9), 9948–9955 (2012).

1. Introduction

Angle-resolved light scattering (ARLS) measurements enable access to information about the morphological and optical properties of scatters such as the refractive index (RI), size, and shape; it has been widely used in research fields including analytical chemistry, biotechnology, and material science [1–3]. Traditionally, ARLS has been measured using goniometer-based instruments; thus, it is challenging to measure the ARLS using microscopic samples. Recently, Fourier transform light scattering (FTLS) was introduced to highly sensitively measure the ARLS signal from microscopic samples [4]. In FTLS, the ARLS signal from individual scatters is obtained through numerically propagating the scalar electric field (*E* field) of the samples to the far fields, which is usually measured using quantitative phase imaging (QPI) techniques [5, 6]. The capability and sensitivity of FTLS has been demonstrated in several studies, including biological samples [7–10], colloidal clusters [11], and solar cells [12]. However, the FTLS technique only measures the ARLS at a fixed wavelength and does not provide spectral information about the scattering signal. This constraint is unfortunate because spectral light scattering can provide abundant information about the scatters. Although several systems have measured angle-resolved or wavelength-dependent light scattering from individual samples [13–20], the simultaneous measurement of the spectro-angular light scattering from individual micrometer-sized samples has not been

#204055 - $15.00 USD Received 2 Jan 2014; revised 8 Feb 2014; accepted 9 Feb 2014; published 13 Feb 2014

demonstrated, primarily due to the technical limitations including unavoidable azimuthal averaging, detector translation, and separate spectral channels for measuring each angular signal.

In this study, a novel light scattering measurement technique, referred to as swept source Fourier-transform light scattering (ssFTLS), is presented and it measures the spectro-angular light scattering. Using the principles of spectroscopic QPI [21] and FTLS [4], the ssFTLS measures the 2D ARLS from individual micrometer-sized samples with a spectral range of 450-750 nm and an angular range of –70-70°. The spectral and angular resolutions are less than 8 nm and 10 mrad, respectively. In addition, the optical phase information of the 2D ARLS is also obtained. The capability of ssFTLS is demonstrated through measuring the spectro-angular light scattering from individual polystyrene microspheres in a phosphate buffered saline (PBS) solution and a bovine serum albumin (BSA) solution.

2. Methods and results

2.1. Swept source Fourier-transform light scattering (ssFTLS)

ssFTLS employs the principle of spectroscopic QPI and FTLS. Spectroscopic QPI measures the *E* fields from a sample in the sample plane with various wavelengths, i.e. $U(x,y;\lambda)$. Then, the far-field scattering signals (U_s) are calculated by numerically propagating the measured *E* fields to the far-field scattering plane. In FTLS, the scattered *E* field U_s at the far-field and the *E* field in the sample plane are related using the Fourier transform, as follows:

$$U_s\left(k_x,k_y;\lambda\right)=\frac{1}{2\pi}\iint U\left(x,y;\lambda\right)\exp\left[-j\left(k_x x+k_y y\right)\right]dxdy\,, \tag{1}$$

where λ is the wavelength of an illumination and k is the lateral spatial frequency corresponding to a scattering angle (θ) in a medium using the relationship $k = 2\pi \cdot n_m \cdot \sin\theta/\lambda$ where n_m is the refractive index of the medium.

Several approaches have been reported for the spectroscopic QPI, including ones that use multiple coherent lasers [22], a broadband light source with band-pass filters [23], a wavelength-swept source [21], spectral filtering using a spatial light modulator [24], and spectral analysis of low-coherence interferogram [25]. In principle, any spectroscopic QPI technique can be used for ssFTLS. In this study, the swept-source diffraction phase microscopy (ssDPM) [21] was used because it provides a wide spectral range with a high spectral resolution. The ssDPM, which is based on common-path full-field interferometric microscopy [5, 6], has a wavelength-swept source and it can measure multispectral *E* field imaging in the visible spectrum with a spectral range of 450-750 nm and an angular range of –70-70°. The lateral spatial resolution of the ssDPM is limited by diffraction, which is approximately 300 nm. The detailed experimental setup for ssDPM has been described elsewhere [21].

The procedure of ssFTLS is depicted in Fig. 1. First, using ssDPM, the holograms of a sample are recorded at various wavelengths [Fig. 1(a)], from which the *E* fields that contain both the amplitude and phase information are retrieved using a field-retrieval algorithm [26] [Fig. 1(b)]. Then, the 2D ARLS is calculated for each wavelength using FTLS [Fig. 1(c)]. Then, the spectro-angular light scattering intensity signals ($|U_s(k_x,k_y;\lambda)|^2$) can be obtained and plotted as a function of the scattering angle and wavelength after averaging in the azimuthal direction [Figs. 1(d) and 1(e)]. In general, ssFTLS can be used to measure 2D spectro-angular light scattering for samples with arbitrary shapes. However, only spherical samples were used in this study for simplicity without losing generality

#204055 - $15.00 USD Received 2 Jan 2014; revised 8 Feb 2014; accepted 9 Feb 2014; published 13 Feb 2014

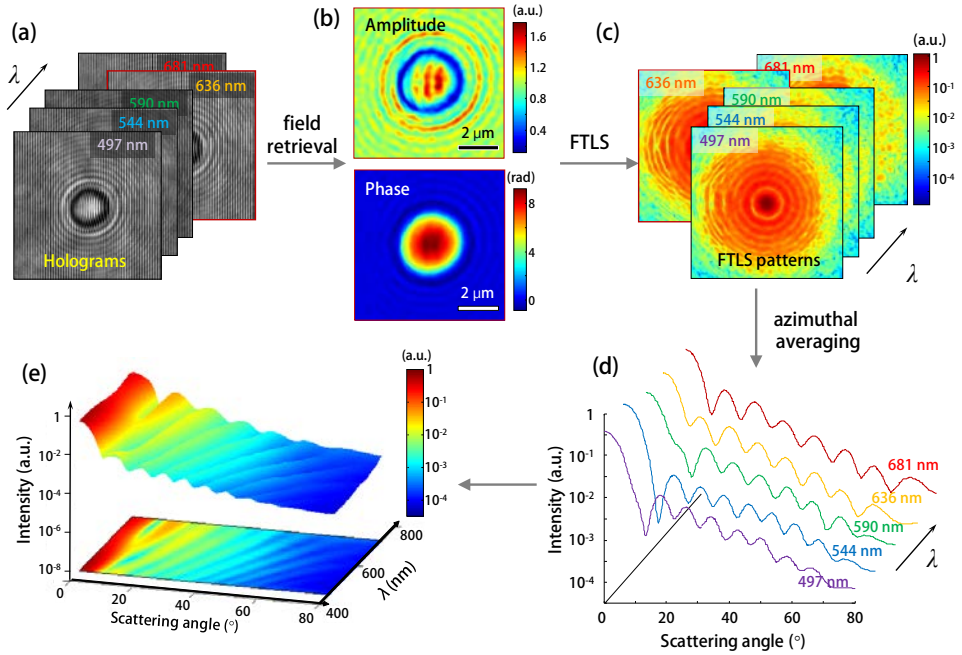

Fig. 1. ssFTLS procedure for measuring the spectro-angular light scattering. (a) The holograms of a sample are recorded at various wavelengths; (b) the corresponding optical fields are obtained using an appropriate retrieval algorithm; (c) the angle-resolved scattering signals at each wavelength are calculated using FTLS; and the scattering signals are presented as a function of the (d) scattering angle and (e) wavelength after averaging in the azimuthal direction.

2.2. Spectro-angular light scattering intensity of individual micro-sized beads

In order to demonstrate the feasibility and capability of ssFTLS, the spectro-angular light intensity scattering patterns of individual microspheres were measured. First, polystyrene microspheres (diameter = 3.0 μm; Invitrogen Inc., USA) that were submerged in a PBS solution were measured according the procedure described in Section 2.1. The measured spectro-angular light scattering patterns of the individual polystyrene beads are presented in Fig. 2(a). The ARLS signals at each wavelength demonstrate a characteristic oscillatory behavior.

In order to test the validity of the measurement, the measured scattering patterns were compared with the numerical simulation based on the Mie scattering theory [27]. The theoretical result is presented in Fig. 2(b). The measured result was consistent with the theoretical scattering signal over the full range of wavelengths and scattering angles [Fig. 2(c)]. In particular, the scattering angles that corresponded to the local minima of the scattering signals were well matched for both the experiments and theory, as indicated by the arrowhead in Fig. 2(c). Furthermore, the extremely low values in the standard deviation imply excellent sensitivity and repeatability of the proposed system. Although the measured scattering intensities are slightly lower than the Mie calculation in the short wavelengths, the oscillatory features in the scattering signal remain in good agreement with the theory. In this system, the deviation may result from an uncorrected chromatic aberration. (Note that all optical lenses used in this system are achromatic.)

In order to demonstrate the sensitivity of the proposed system, the spectro-angular light scattering of the polystyrene beads was measured after changing the surrounding medium from a PBS solution to 30% BSA solution (300 mg/ml). Then, the experiments were repeated for nine individual beads. As seen in Fig. 3, the measured and theoretical results are consistent

#204055 - $15.00 USD Received 2 Jan 2014; revised 8 Feb 2014; accepted 9 Feb 2014; published 13 Feb 2014

over the full spectro-angular domain. Although the refractive index difference between the PBS and BSA solution was small (0.041 ± 0.001 for the spectral range of 450-750 nm), ssFTLS measured the spectro-angular light scattering with unprecedented precision and sensitivity.

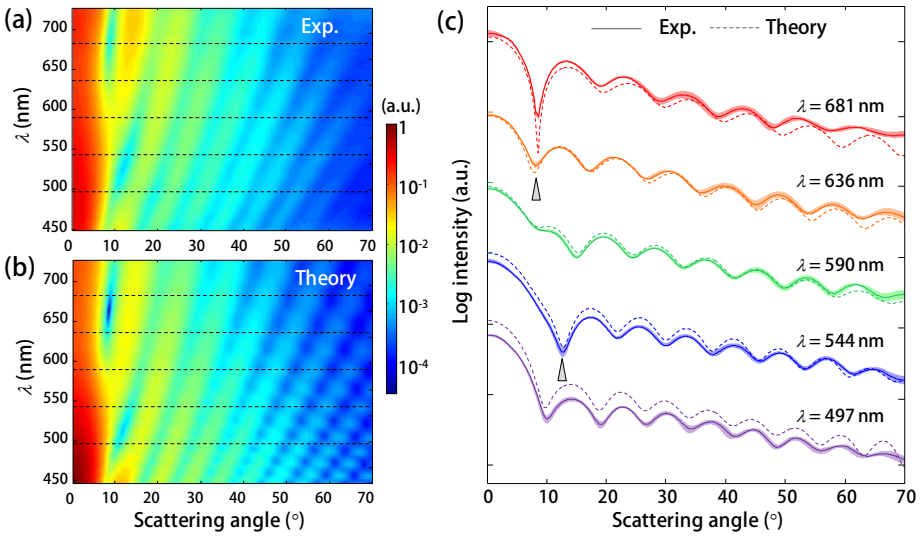

Fig. 2. Spectro-angular light scattering measurements of a polystyrene bead submersed in a PBS solution. (a) The average scattering intensity of nine samples measured using ssFTLS; (b) the theoretical scattering intensity calculated using the Mie theory; and (c) for comparison, the experimental results from (a) and the theory from (b) are plotted together at five representative wavelengths [i.e. the black dashed lines in (a) and (b)]. The color-shaded areas represent the standard deviations for the nine measurements.

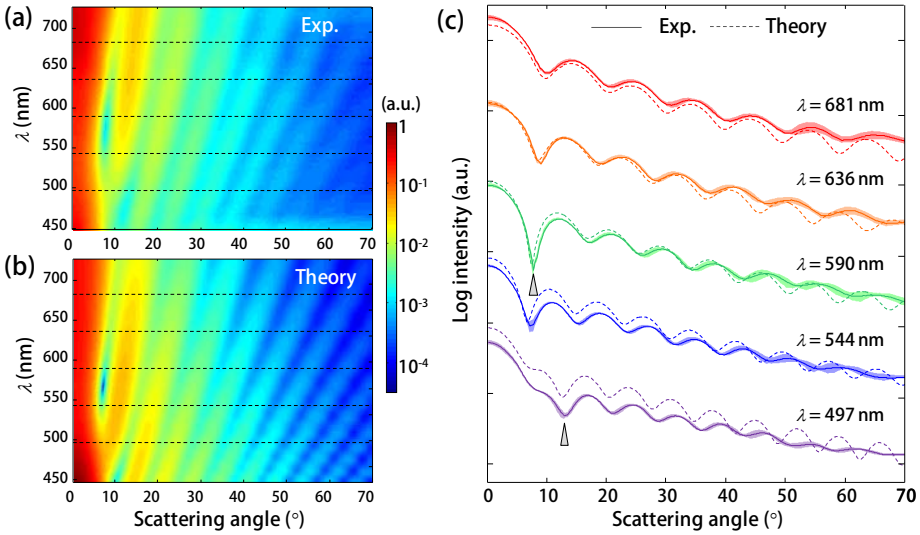

Fig. 3. Spectro-angular light scattering measurement of a polystyrene bead submersed in the BSA solution. (a) The average scattering intensity of the nine samples measured using ssFTLS; (b) the theoretical scattering intensity calculated using the Mie theory; and (c) for comparison, the experimental results from (a) and the theory from (b) are plotted together at five representative wavelengths [i.e. the black dashed lines in (a) and (b)]. The color-shaded areas represent the standard deviations for the nine measurements.

#204055 - $15.00 USD Received 2 Jan 2014; revised 8 Feb 2014; accepted 9 Feb 2014; published 13 Feb 2014

2.3. Optical phase of the spectro-angular light scattering

The optical phase information of the spectro-angular light scattering can also be retrieved using ssFTLS. Because the complex amplitude of the scattered light fields are obtained in FTLS as follows,

$$U_s\left(k_x,k_y;\lambda\right)=\left|U_s\left(k_x,k_y;\lambda\right)\right|\exp\left[\,j\phi(k_x,k_y;\lambda)\right], \tag{2}$$

where the phase information of the scattered field $\phi(k_x,k_y;\lambda)$ is readily available because $\phi(k_x,k_y;\lambda) = \angle U_s(k_x,k_y;\lambda)$. The optical phase of the scattering signal contains information about the position and morphology of the samples [28]. However, due to the lack of measurement techniques, the optical phase of the scattering has not been explored sufficiently: only the optical phase of scattering from a bulk sample has been measured [29].

The optical phase maps of the spectro-angular light scattering from an individual polystyrene bead in the PBS and 30% BSA solutions are presented in Figs. 4(a) and 4(c), respectively. The measured optical phase maps are consistent with the numerical simulations based on the Mie theory [Figs. 4(b) and 4(d) for the PBS and BSA solutions, respectively]. To date, this is the first reported experimental measurement of the optical phases of scattered fields from individual scatters. The capability of optical phase measurement in the ssFTLS method can be used to precisely investigate changes in the position and shape of micrometer-sized samples.

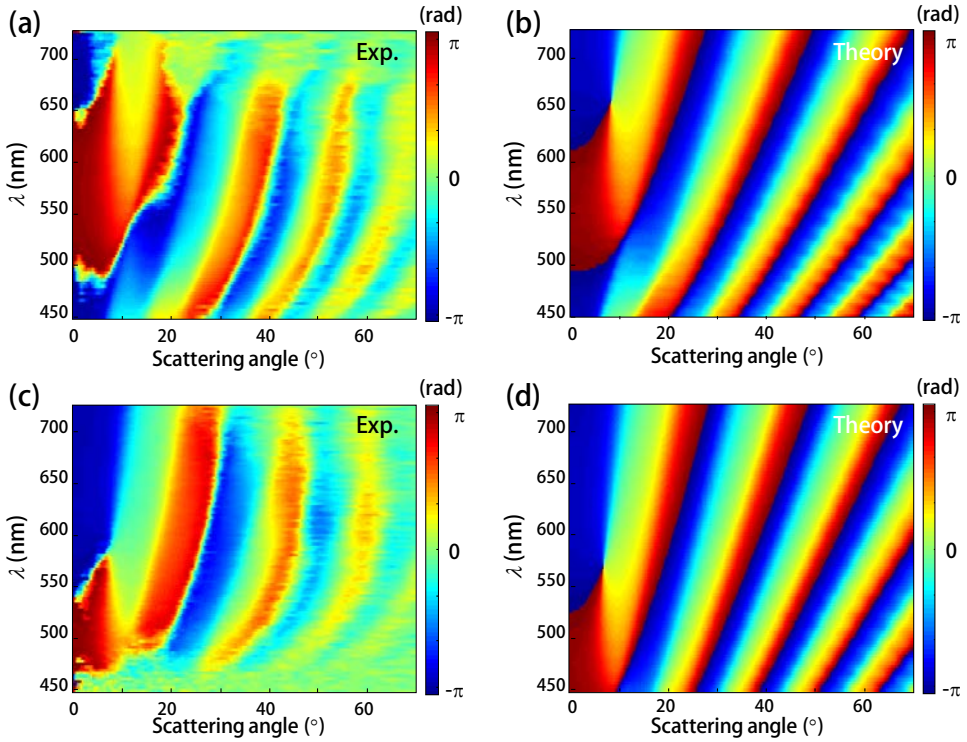

Fig. 4. The optical phases of the spectro-angular light scattering. (a) and (b) The optical phase of the spectro-angular light scattering from a polystyrene bead submersed in a PBS solution (a) measured using ssFTLS and (b) calculated from the Mie theory. (c) and (d) The optical phase of the spectro-angular light scattering from a polystyrene bead submersed in a 30% BSA solution (c) measured using ssFTLS and (d) calculated from the Mie theory.

#204055 - $15.00 USD Received 2 Jan 2014; revised 8 Feb 2014; accepted 9 Feb 2014; published 13 Feb 2014

3. Discussions and conclusions

A method has been proposed for measuring the spectro-angular light scattering from individual microscopic objects. Using the principle of spectroscopic QPI and FTLS, the quantitative and precise measurements of spectro-angular light scattering from polystyrene microbeads were demonstrated. It was also demonstrated that the optical phase of the spectro-angular light scattering could be obtained. The measured spectro-angular light scattering intensity and phase patterns were well matched with the Mie theory.

In this study, the light scattering signal was obtained in the spectrum over 450-750 nm with a spectral resolution of less than 8 nm and in the scattering angle over –70-70° (–1.22 to 1.22 rad) with an angular resolution of less than 0.5° (10 mrad). The spectral range and resolution were determined using a light source and a wavelength-sweeping unit, respectively, which could be further enhanced using high-power wide-spectrum illumination (e.g. a supercontinuum laser). Furthermore, although the present ssFTLS has been demonstrated in visible wavelengths, it can be easily adapted for other spectral ranges. For example, through only modifying a part of the wavelength-swept source, the wavelength ranges can be adjusted from ultraviolet (UV) to visible and to infrared (IR). Hyper-spectral ssFTLS measurements are also possible. The scattering angle range is primarily limited through the numerical aperture of the objective lens, and the angular resolution is determined using the field-of-view in the QPI system. However, it can be further extended using an aperture-synthesis technique [30].

The temporal resolution of ssFTLS is primarily determined using the repetition rate of the wavelength-swept part. In the present system, the temporal resolution is approximately 5 s for one full spectro-angular measurement, which is limited due to the low spectral density of the light source used. However, the temporal resolution of the ssFTLS can be further enhanced using a high power source, and it may enable the investigation of dynamic spectro-angular light scattering measurements.

It is expected that ssFTLS can be used in various applications including surface inspections, resonance light-matter interactions in metallic nanostructures, and chemical compositions through the unprecedented spectro-angular resolving capability. Structural characteristics in nanoscale could be determined with high sensitivity and accuracy through a wealth of information from spectro-angular light scattering measurements [13, 16]. In particular, the analysis and study of spectro-angular light scattering from biological cells and tissues may enable investigations of the pathophysiology of several diseases such as malaria and sickle cell disease [31–35]. In addition, the incorporation of ssFTLS into a commercial microscope is possible and straightforward using the principle of inline holography [36]. Furthermore, when combined with a polarization-sensitive QPI technique [37], ssFTLS could be extended to investigate the spectro-angular light scattering of optically anisotropic samples.

Acknowledgments

This work was supported by KAIST, the Korean Ministry of Education, Science and Technology (MEST), and the National Research Foundation (2012R1A1A1009082, 2013K1A3A1A09076135, 2013M3C1A3063046, 2009-0087691, 2012-M3C1A1-048860).